Golgi and plasma membrane pools of PI(4)P contribute to plasma membrane PI(4,5)P$_2$ and maintenance of KCNQ2/3 ion channel current

Eamonn J. Dickson, Jill B. Jensen, and Bertil Hille[1]

Department of Physiology and Biophysics, University of Washington School of Medicine, Seattle, WA 98195

Plasma membrane (PM) phosphatidylinositol 4,5-bisphosphate [PI(4,5)P$_2$] regulates the activity of many ion channels and other membrane-associated proteins. To determine precursor sources of the PM PI(4,5)P$_2$ pool in tsA-201 cells, we monitored KCNQ2/3 channel currents and translocation of PH$_{PLC\delta1}$ domains as real-time indicators of PM PI(4,5)P$_2$, and translocation of PH$_{OSH2\times2}$, and PH$_{OSH1}$ domains as indicators of PM and Golgi phosphatidylinositol 4-phosphate [PI(4)P], respectively. We selectively depleted PI(4)P pools at the PM, Golgi, or both using the rapamycin-recruitable lipid 4-phosphatases. Depleting PI(4)P at the PM with a recruitable 4-phosphatase (Sac1) results in a decrease of PI(4,5)P$_2$ measured by electrical or optical indicators. Depleting PI(4)P at the Golgi with the 4-phosphatase or disrupting membrane-transporting motors induces a decline in PM PI(4,5)P$_2$. Depleting PI(4)P simultaneously at both the Golgi and the PM induces a larger decrease of PI(4,5)P$_2$. The decline of PI(4,5)P$_2$ following 4-phosphatase recruitment takes 1–2 min. Recruiting the endoplasmic reticulum (ER) toward the Golgi membranes mimics the effects of depleting PI(4)P at the Golgi, apparently due to the *trans* actions of endogenous ER Sac1. Thus, maintenance of the PM pool of PI(4,5)P$_2$ appears to depend on precursor pools of PI(4)P both in the PM and in the Golgi. The decrease in PM PI(4,5)P$_2$ when Sac1 is recruited to the Golgi suggests that the Golgi contribution is ongoing and that PI(4,5)P$_2$ production may be coupled to important cell biological processes such as membrane trafficking or lipid transfer activity.

phosphoinositides | wortmannin | pleckstrin homology domain

This paper concerns the dynamics of cellular pools of phosphoinositides, a family of phospholipids located on the cytoplasmic leaflet of cellular membranes, that maintain cell structure, cell motility, membrane identity, and membrane trafficking; they also play key roles in signal transduction (1). Phosphatidylinositol (PI) can be phosphorylated at three positions to generate seven additional species. The subcellular localization of each phosphoinositide is tightly governed by the concurrent presence of lipid kinases and lipid phosphatases (2, 3), giving each membrane within the cell a unique and dynamic phosphoinositide signature (4). Phosphatidylinositol 4,5-bisphosphate [PI(4,5)P$_2$] is localized to the inner leaflet of the plasma membrane (PM) and is the major substrate of phospholipase C (PLC). As a consequence, PI(4,5)P$_2$ levels are dynamically regulated by G$_q$-coupled receptors activating PLC. The activity of lipid kinases and phosphatases also can be modulated by signaling; for example, a PI 4-kinase, when associated with neuronal calcium sensor-1, is accelerated in response to elevated calcium that occurs with PI(4,5)P$_2$ cleavage (5). In addition, transient apposition between organelles can alter phosphoinositide levels by presenting membrane-bound phosphatases *in trans*. For example, the endoplasmic reticulum (ER) can make contacts with the Golgi, allowing 4-phosphatases of the ER to dephosphorylate Golgi phosphatidylinositol 4-phosphate [PI(4)P] (6–8).

PI(4,5)P$_2$ is a dynamically regulated positive cofactor required for the activity of many plasma membrane ion channels (9). Current in KCNQ2/3 channels (the molecular correlate of neuronal M-current)

can be turned off in a few seconds by depletion of PI(4,5)P$_2$ following activation of PLC through G$_q$-coupled M$_1$ muscarinic receptors (M$_1$Rs) (10–12). Given the importance of PI(4,5)P$_2$, we wanted to understand better how it is sourced from its precursor PI(4)P within the cell. How do subcellular compartments influence PI(4,5)P$_2$ abundance at the plasma membrane? PI(4,5)P$_2$ is derived from PI in two steps: PI 4-kinases make PI(4)P, and PI(4)P 5-kinases make PI(4,5)P$_2$. Thus, PI(4)P is the immediate precursor of PI(4,5)P$_2$. Mammalian cells express at least four distinct isoforms of PI 4-kinase that phosphorylate PI on the 4 position to generate PI(4)P and are commonly referred to as PI4K types II (α and β) and III (α and β) (1, 13). PI 4-kinase type IIIα generates PI(4)P at both the Golgi and the PM (14–16). Originally thought to be localized to an ER/Golgi compartment (17, 18), recent experiments show that it is targeted to the plasma membrane by a palmitoylated peripheral membrane protein (16). PI 4-kinase IIIβ is said to be localized to the Golgi and nucleus and contributes to the biosynthesis of Golgi PI(4)P through its association with Arf1 and neuronal calcium sensor 1 (19–21). Inhibition of PI 4-kinase IIIα and -β with micromolar concentrations of wortmannin prevents the replenishment of PM PI(4,5)P$_2$ following PLC activation (10, 22, 23). Type IIα and IIβ PI4Ks are membrane-bound proteins due to the palmitoylation of a conserved stretch of cysteines in their catalytic domains (24). Immunocytochemical analysis has revealed that they are mostly associated with *trans*-Golgi, endoplasmic reticulum, and endosomal membranes (25–27). These type IIα and IIβ enzymes are blocked by adenosine and calcium, but are resistant to wortmannin. Therefore, they are not thought to contribute to the recovery of PM PI(4,5)P$_2$ following G$_q$-receptor activation (10, 24). Our understanding of the contribution of the PI 4-kinase

Significance

Phosphatidylinositol 4,5-bisphosphate [PI(4,5)P$_2$] is a key informational phospholipid, localized to and defining the inner leaflet of the plasma membrane (PM). How PM PI(4,5)P$_2$ is sourced and regulated is critically important to the understanding of cellular trafficking, cell motility, membrane identity, and ion channel activity. The immediate precursor of PI(4,5)P$_2$ is PI(4)P. Direct evidence detailing the location and contribution of PI(4)P pool(s) maintaining steady-state PM PI(4,5)P$_2$ is lacking. We find that PM PI(4,5)P$_2$ levels are supported by at least two continuously supplying precursor pools of PI(4)P, one in the PM and the other in the Golgi. The contribution of the Golgi pool of PI(4)P highlights the possibility that PM PI(4,5)P$_2$ production is coupled to important cell biological processes.

Table 1. Rapamycin inducible dimerization partners

FKBP-construct	Pre-rapamycin localization	FRB-anchor name/ localization	Post-rapamycin FKBP-construct localization	Perturbation	Used in figure
PJ	Cyto.	Lyn$_{11}$-FRB/PM	PM	PM PI(4,5)P$_2$ → PI	Fig. 2, Fig. S2
PJ-5P	Cyto.	Lyn$_{11}$-FRB/PM	PM	PM PI(4,5)P$_2$ → PI(4)P	Fig. 2
PJ-4P	Cyto.	Lyn$_{11}$-FRB/PM	PM	PM PI(4)P → PI	Fig. 2, Fig. S1, Fig. S4
PJ-Dead	Cyto.	Lyn$_{11}$-FRB/PM	PM	No effect	Fig. 2
PJ-4P	Cyto.	Tgn38-FRB/Tgn	Tgn	Tgn PI(4)P → PI	Fig. 3, Fig. S2, Fig. S4
hSac	Cyto.	Tgn38-FRB/Tgn	Tgn	Tgn PI(4)P → PI	Fig. 3
PJ-5P	Cyto.	Tgn38-FRB/Tgn	Tgn	Tgn PI(4,5)P$_2$ →PI(4)P	Fig. 3
PJ-Dead	Cyto.	Tgn38-FRB/Tgn	Tgn	No effect	Fig. 3
PJ-4P	Cyto.	Lyn$_{11}$-FRB & Tgn38-FRB/PM & Tgn	PM & Tgn	PM & Tgn PI(4)P → PI	Fig. 4, Fig. S3
CB5-FKBP	ER	Tgn38-FRB/Tgn	Golgi	ER and Tgn brought into closer proximity	Fig. 7

Cyto., cytoplasm; ER, endoplasmic reticulum; PM, plasma membrane; Tgn, *trans*-Golgi network.

isoforms is undergoing refinement by accumulating information concerning the unique localization, trafficking, and activity of each PI 4-kinase.

Although PI 4-kinase isoforms are present in the membranes of several organelles, the most abundant pools of PI(4)P appear to be those of the PM, Golgi, and secretory vesicles (13–15, 28). A need for Golgi PI(4)P in the maintenance of PM PI(4,5)P$_2$ was indirectly revealed when plasma membrane PI(4,5)P$_2$ recovery was slowed following recruitment of a 4-phosphatase to the *trans*-Golgi network (28). Depletion of PM PI(4)P has been shown to result in small changes to PM PI(4,5)P$_2$ (15, 22), and knockout of the PM-bound PI 4-kinase IIIα resulted in loss of PI(4)P and a relocation of PI(4,5)P$_2$ biosensors to intracellular membranes (16). Nevertheless, others have proposed that PM PI(4)P is redundant for the synthesis of PM PI(4,5)P$_2$ (29–31) and may not serve as its immediate precursor because treatment with the type III PI 4-kinase inhibitor wortmannin or recruiting a 4-phosphatase to the PM had little effect on the PM localization of the PI(4,5)P$_2$ reporter, the pleckstrin homology (PH) domain from PLCδ1 (PH$_{PLCδ1}$).

Here, we revisit the relative contributions of PI(4)P pools to PM PI(4,5)P$_2$. We find that the majority of PM PI(4,5)P$_2$ needed for maintenance of KCNQ currents comes from two precursor pools of PI(4)P in the cell, one in the PM and the other in the Golgi. The PM pool makes the larger contribution, but the contribution from both locations is significant and ongoing.

Results

Phosphatase Tools to Deplete Specific Phosphoinositide Pools. Assessing potential precursor sources for plasma membrane PI(4,5)P$_2$ required effective ways to deplete specific phosphoinositide pools. We recruited lipid phosphatase enzymes to specific membrane anchors using drug-induced dimerization. Enzymes coupled to FK506 binding protein (FKBP) and membrane anchors coupled to FKBP-rapamycin binding domain (FRB) were dimerized by the addition of rapamycin. (see listing in Table 1). We focused on the two membranes most likely to contribute to the maintenance of PM PI(4,5)P$_2$, the plasma membrane (using the Lyn$_{11}$ anchor) and the Golgi [using the *trans*-Golgi network 38 (Tgn38) anchor]. The experiments used four lipid-phosphatase constructs related to pseudojanin (PJ) (29) (Fig. 1). They are the dual phosphatase PJ itself, which is an engineered tandem of a 5-phosphatase (INPP5E) and a 4-phosphatase (Sac1), and its three point-mutant variants with only the 4-phosphatase active (abbreviated as PJ-4P), with only the 5-phosphatase active (PJ-5P), and with both lipid phosphatases inactivated (PJ-Dead). Of these, PJ-4P was used the most often here, as after recruitment to a membrane by rapamycin it would remove the 4-phosphate from PI(4)P to produce PI. Note

that the Sac1 enzyme has diverse substrate selectivity, being able to dephosphorylate PI(3)P, PI(4)P, and PI(3,5)P$_2$ [but not PI(4,5)P$_2$] into PI (32, 33). Because PI(4)P is more abundant than the other Sac1 substrates within the plasma and *trans*-Golgi membranes, we use a simplified and imprecise notation, calling the PJ construct that contains only Sac1, PJ-4P. Sometimes we call the unmutated version of PJ "full PJ" to emphasize that it is an active dual phosphatase. Each translocatable phosphatase construct had a fluorescent protein [red fluorescent protein (RFP) or YFP] and a FKBP domain at its N terminus and was localized primarily to the cytoplasm when expressed in tsA-201 cells (e.g., confocal micrograph in Fig. 2A).

Recruiting Sac1 Phosphatase to the Plasma Membrane Reduces PM PI(4)P and PI(4,5)P$_2$. The logic of our experiments with PJ-4P can be understood by reference to the reaction schemes and cartoons at the *Top* of Fig. 2A. In preliminary experiments, we tested the tandem PH domains of oxysterol-binding protein homolog 2 (PH$_{OSH2×2}$) to see if it is a specific monitor of PM PI(4)P (Table 2). There are differing reports regarding the selectivity of oxysterol-binding protein homologs (OSH) proteins for PM PI(4)P. A construct with a single PH$_{OSH2}$ domain has been used to report both PI(4)P and PI(4,5)P$_2$ in vitro (34, 35) but also has been used to monitor PI(4)P levels in mammalian cell lines (16). On the other hand, the tandem PH$_{OSH2×2}$ probe is considered more selective for PM PI(4)P (14, 36–38). Indeed, two observations suggest that the PH$_{OSH2×2}$ probe has greater sensitivity to PM PI(4)P over PM PI(4,5)P$_2$. First, we find that recruitment of PJ-5P to the PM, which dephosphorylates PI(4,5)P$_2$ into PI(4)P, caused a small increase in PH$_{OSH2×2}$ probe intensity at the PM (Fig. S1A). Second, following the addition of rapamycin and consequent recruitment of PJ-4P to the PM anchor (LDR: N-terminal sequence of Lyn kinase coupled to FRB domain), the PH$_{OSH2×2}$ intensity decreased at the PM and increased concurrently in the cytoplasm (Table 1 and Fig. S1B). Such observations are consistent with the concept that PH$_{OSH2×2}$ monitors PM PI(4)P, but do not unequivocally rule out some interaction with PM PI(4,5)P$_2$.
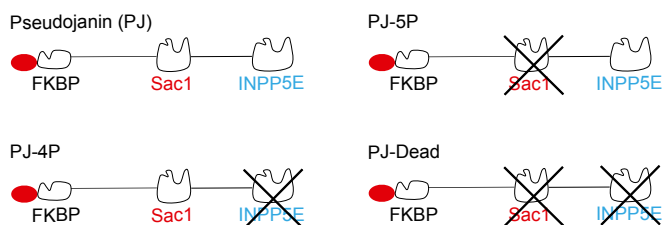
Table 2. Lipid indicator domains

Name	Used as indicator for:	Localization in resting cell	Figure in text
PH$_{PLCδ1}$	PM PI(4,5)P$_2$	PM	Fig. 2
PH$_{OSH2x2}$	PM PI(4)P	PM	Fig. S1
PH$_{OSH1}$	Tgn PI(4)P	Tgn	Figs. 3 and 7; Fig. S4
ING2	PI(5)P	Cytoplasm	Fig. S1

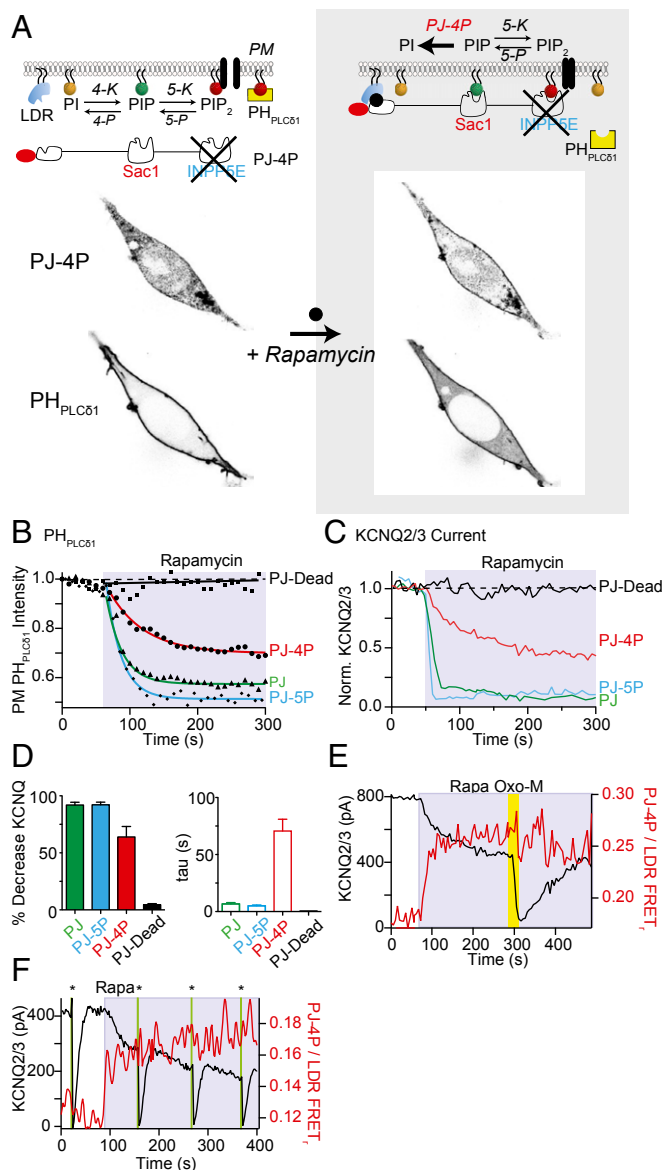Cyto., cytoplasm; Tgn: *trans*-Golgi network; PM, plasma membrane.

Because the enzymatic selectivity of PJ-4P has no such ambiguity and dephosphorylates only PI(4)P, and not PI(4,5)P$_2$, into PI (32), we decided to test for a PM pool of PI(4)P contributing to PM PI(4,5)P$_2$ by monitoring PM PI(4,5)P$_2$ directly using a PH$_{PLC\delta1}$ probe (Table 2) and by recruiting PJ-4P. Consistent with the concept of a PM precursor pool of PI(4)P, the addition of rapamycin and recruitment of PJ-4P to the PM led to a decrease in PH$_{PLC\delta1}$ intensity at the PM (Fig. 2A). This decrease of PM PI(4,5)P$_2$ after recruiting PJ-4P was slower (exponential time constant: $\tau = 61$ s) than that after recruiting either the full PJ or PJ-5P, which cleave PI(4,5)P$_2$ directly ($\tau = \sim10$ s; Fig. 2B). We suggest that the delayed decrease in PM PH$_{PLC\delta1}$ intensity, following PJ-4P recruitment, represents a secondary decline of PM PI(4,5)P$_2$ following depletion of a precursor PM pool of PI(4)P.

Two control experiments provided further evidence that the slow decrease in PH$_{PLC\delta1}$ intensity is due to selective depletion of a PM PI(4)P pool and not to direct dephosphorylation of PI(4,5)P$_2$ or to an effect of rapamycin recruitment alone. First, we used a fluorescent probe for PI(5)P PH (GFP-ING2-PH, Table 2) (39). If PJ-4P were able to remove a phosphate from the 4 position of PI(4,5)P$_2$, it would be expected to generate PI(5)P at the PM. However, with recruitment of PJ-4P to the PM there was no change in intensity of GFP-ING2-PH at the PM (Fig. S1C). As a positive control of the probe, dialysis of 5 μM diC$_8$ D-myo-phosphatidylinositol 5-phosphate [PI(5)P] into the same cell via a patch pipette did result in an increase in PM GFP-ING2-PH intensity (Fig. S1). This experiment fully supports the existing literature detailing the inability of Sac1 to dephosphorylate PI(4,5)P$_2$ directly. Second, recruiting the inactive PJ-Dead to the PM resulted in no change in PH$_{PLC\delta1}$ intensity (Fig. 2B). Collectively, these results provide evidence that (*i*) recruiting PJ-4P to the PM directly dephosphorylates a PM pool of PI(4)P and that (*ii*) this PM pool is a precursor for the generation and maintenance of PM PI(4,5)P$_2$.

PM PI(4)P Makes a Large Contribution to PM PI(4,5)P$_2$ and KCNQ2/3 Currents. KCNQ2/3 channels require PI(4,5)P$_2$ as a cofactor for function. We used these channels as a sensitive monitor of PM PI(4,5)P$_2$. Replacing RFP with YFP on the N-terminal of the PJ construct allowed us to measure the Förster resonance energy transfer (FRET) between PJ and a membrane anchor (YFP-PJ-4P, acceptor; LDR-CFP, anchor and donor). An increase in FRET ratio (FRET$_r$) would indicate positive recruitment of PJ-4P to the intended membrane of interest (Fig. 2 *E* and *F* and Fig. S2). Recruiting YFP-PJ-Dead to the PM anchor LDR-CFP consistently produced both an increase in acceptor fluorescence YFP$_C$ and a decrease in the donor fluorescence CFP$_C$, reflecting recruitment as an increase in FRET$_r$, but no change in KCNQ2/3 currents (Fig. 2C, solid black line). Rapamycin-induced recruitment of either YFP-PJ-5P (Fig. 2C, blue line) or YFP-PJ (Fig. 2C, green line) to the PM-initiated rapid increases in FRET$_r$ (translocation) and also very rapid reduction in KCNQ2/3 currents

Fig. 2. Recruiting pseudojanin 4- and 5-phosphatases to the plasma membrane reduces plasma membrane PI(4,5)P$_2$ and KCNQ2/3 current. (*A*) Schematic representation of PI(4)P depletion by pseudojanin-Sac (PJ-4P) recruitment to the PM. PI, phosphatidylinositol; PIP, phosphatidylinositol 4-phosphate; PIP$_2$, phosphatidylinositol 4,5-bisphosphate; PH$_{PLC\delta1}$, pleckstrin homology domain of phospholipase Cδ1; Sac1, 4-phosphatase; INPP5E, 5-phosphatase. Recruitment of PJ-4P to the plasma membrane reduces PI(4,5)P$_2$ levels at the plasma membrane. Inverted confocal micrographs of RFP-PJ-4P and PH$_{PLC\delta1}$ distribution before (*Left*) and after (*Right*) 5 μM rapamycin. (*B*) Averaged normalized time courses (symbols; $n = 7$) and single-exponential fits (solid lines) of plasma membrane PH$_{PLC\delta1}$ intensity following recruitment of PJ enzymes to plasma membrane with the addition of 5 μM rapamycin. PJ (triangles, green line); PJ-4P, PJ with 4-phosphatase only (INPP5E inactivated; circles, red line); PJ-5P, PJ with 5-phosphatase only (Sac inactivated; diamonds, blue line); PJ-Dead, mutant PJ with both phosphatases inactivated (squares, black line). (*C*) Averaged normalized time courses ($n = 6$) of KCNQ2/3 current with 5 μM rapamycin. (*D*) Summary of percentage decrease of KCNQ2/3 current (*Left*) and time constants of single-exponential fits (*Right*) after recruitment of four enzymes. (*E*) Averaged time courses of KCNQ2/3 current (left axis, black line) and FRET$_r$ between YFP-PJ-4P and LDR-CFP (right axis, red line) with application of 5 μM rapamycin and 10 μM oxotremorine-M. M$_1$ muscarinic receptor is coexpressed. (*F*) Averaged time courses of KCNQ2/3 current (left axis, black line) and FRET$_r$ (right axis, red line) with application of 5 μM rapamycin and four activations of voltage-sensitive phosphatase by 1-s depolarizations to +100 mV (asterisks).

Fig. 1. Diagram of the four pseudojanin constructs and their names. PJ: engineered tandem 5-phosphatase (INPP5E) and 4-phosphatase (Sac1). PJ-4P: Only the 4-phosphatase is catalytically active. PJ-5P: Only the 5-phosphatase is active. PJ-Dead: Both enzymes are catalytically inactive. Each construct has an RFP (red oval) and FKBP domain at its N terminus.

by ∼90% (τ of KCNQ inhibition: PJ = 13 s; PJ-5P = 10 s; Fig. 2 C and D). The decreases of KCNQ2/3 current with recruitment of PJ or PJ-5P report the dephosphorylation of PM PI(4,5)P$_2$ at the 5 position. When, instead, PJ-4P was recruited to the PM, we found that KCNQ2/3 currents were reduced by only ∼60%, starting at once but at a much slower rate than with either PJ or PJ-5P (τ of KCNQ inhibition with PJ-Sac = 141 s; Fig. 2 C–F). Once KCNQ2/3 currents had reached a new steady-state level, the remaining PI(4,5)P$_2$ could still be depleted by activation (i) of PLC through the M$_1$R agonist Oxo-M (10 μM) or (ii) of voltage-sensitive phosphatase (VSP) (Fig. 2 E and F). Note that KCNQ2/3 tail currents subsequently recovered to a similar level as before either M$_1$R or VSP activation. These experiments are compatible with a significant plasma membrane pool of PI(4)P that helps maintain the PM PI(4,5)P$_2$ pool that supports KCNQ2/3 currents. They also suggest that there could be additional sources of PI(4)P in locations other than the PM because KCNQ2/3 currents do not fall to zero and recovery from PI(4,5)P$_2$ depletion still occurs. We next consider the Golgi as an additional source for maintaining PM PI(4,5)P$_2$.

Recruiting Sac1 Phosphatase to the Golgi Depletes Golgi PI(4)P. A classical source of PI(4)P is the Golgi (40, 41). Several PH-domain probes have high in vitro specificity for Golgi PI(4)P including the four-phosphate-adaptor protein (FAPP) 1, the oxysterol-binding protein (OSBP), and the oxysterol-binding protein homologs (OSH). These probes report PI(4)P well in the Golgi because they also require Arf1-GTP, which is located at the Golgi. Here we use PH$_{OSH1}$ as the reporter of Golgi PI(4)P, but preliminary experiments with the other PI(4)P probes gave similar results.

Under controlled expression conditions (*Materials and Methods*), PH$_{OSH1}$ was tightly localized to the *trans*-Golgi network (Fig. 3A). Recruiting the cytosolic PJ-4P to the *trans*-Golgi network anchor Tgn38-FRB-CFP (Table 1) resulted in a decline in the intensity of the Golgi PI(4)P reporter PH$_{OSH1}$ (Fig. 3A and red line in Fig. 3B; Movie S1) with a time constant of $\tau = 61$ s. The reduction of PH$_{OSH1}$ over the Golgi parallels the increase in PJ-4P intensity over the same region of interest (Fig. 3A). To validate the actions of the yeast Sac1 domain in the PJ-4P construct, we performed confocal time series experiments while recruiting a truncated human Sac1 4-phosphatase (hSac1$_{tr}$) to Tgn38. The hSac1$_{tr}$ enzyme was cytoplasmic because the ER-localizing transmembrane segments were absent (28). As with PJ-4P, rapamycin induced an increase in mRFP-FKBP-hSac1$_{tr}$ intensity and a decrease in PH$_{OSH1}$ over the same region of interest (Fig. 3B, dashed orange line). The time constant for PH$_{OSH1}$ release from the Golgi to the cytosol was similar for the two Sac constructs (Fig. 3B). The functional similarity between actions of yeast and human Sac1 is consistent with the high degree of sequence similarity between the Sac1 orthologs (33, 42). The fluorescence intensity of PH$_{OSH1}$ remained unchanged following recruitment of PJ-Dead to the Golgi (Fig. 3B).

Previous quantitative analysis of the trafficking patterns of Tgn38 (our Golgi anchor) revealed an apparent steady-state distributed between the *trans*-Golgi network (∼80%), plasma membrane (∼10%), and recycling endosomes (∼10%) (43). Therefore, in our experiments we selected cells that had a predominance of Tgn38-FRB-CFP localized to the *trans*-Golgi with little detectable expression at the PM or other cytoplasmic structures. Nevertheless, as an important control to verify proper Golgi targeting, we used the Tgn38-FRB-CFP anchor to recruit the powerful 5-phosphatase PJ-5P (Fig. 3C). Addition of rapamycin led to only minor changes in the KCNQ2/3 tail current (<5%), allowing us to conclude that the fraction of this anchor residing in the PM under our controlled expression conditions is too small to bias our results. Together, our data so far suggest that PJ-4P can be used to reduce PI(4)P levels selectively either at the PM or at the Golgi. With this background, we now can ask what
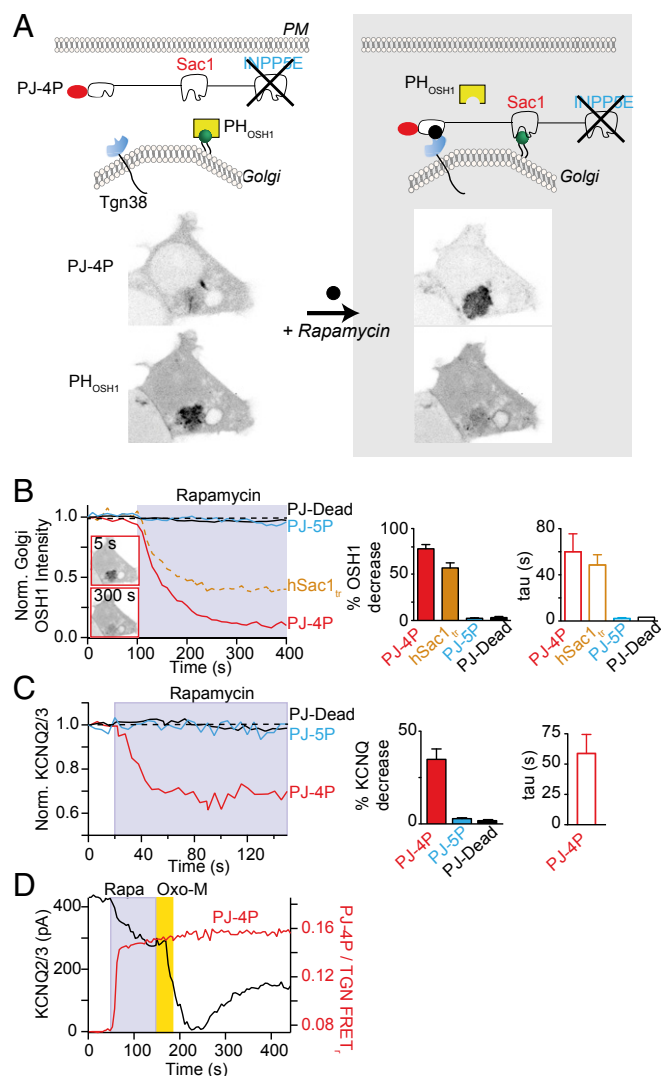
Fig. 3. Recruiting pseudojanin 4-phosphatase to the Golgi reduces Golgi PI(4)P and plasma membrane KCNQ2/3 current. (A) Schematic of PI(4)P depletion following PJ-4P recruitment to the Golgi. OSH1, oxysterol-binding protein homolog 1. Inverted confocal images of PJ-4P and PH$_{OSH1}$ before and after 5 μM rapamycin. (B) Averaged normalized time courses ($n = 7$) of the Golgi intensity of the PI(4)P probe OSH1 with addition of 5 μM rapamycin in the presence of each of the four recruitable PJ enzymes. (*Inset*) Inverted confocal images of a representative cell before (*Upper*) and during (*Lower*) the recruitment of PJ-4P by rapamycin. Note same cell as in A. (*Right*) Summary of percentage decrease of OSH1 Golgi intensity and time constants (tau) of single-exponential fits after enzyme recruitment. (C) Averaged normalized time courses of KCNQ2/3 current with addition of 5 μM rapamycin in the presence of three Golgi-targeted enzymes. (*Right*) Summary of percentage decrease of KCNQ2/3 current (*Left*) and time constants of single-exponential fits (*Right*) after enzyme recruitment. (D) Averaged time courses of KCNQ2/3 current (left axis, black line) and FRET$_r$ between YFP-PJ-4P and LDR-CFP (right axis, red line) with application of 5 μM rapamycin and 10 μM oxotremorine-M. M$_1$ muscarinic receptor is coexpressed.

effect depleting Golgi PI(4)P has on the PM pool of PI(4,5)P$_2$ that supports KCNQ2/3 channel activity.

Golgi PI(4)P also Contributes to PM PI(4,5)P$_2$. To deplete Golgi PI(4)P pools, we recruited the YFP-PJ-4P enzyme to Tgn38-FRB-CFP. At the same time, we monitored FRET as an indicator of translocation of YFP-PJ-4P and recorded PM KNCQ2/3 currents as a reporter of PM PI(4,5)P$_2$ levels. Upon the addition of rapamycin, cytosolic YFP-PJ-4P was reliably recruited to the *trans*-Golgi

as indicated by increasing FRET$_r$ (Fig. 3D and Fig. S2). A concurrent slow ~30% decrease in KCNQ2/3 tail currents (Fig. 3C, red line; $\tau = 59$ s) suggested that Golgi PI(4)P contributes to PI(4,5)P$_2$ synthesis at the PM. Following muscarinic receptor activation of PLC, the remaining PI(4,5)P$_2$ was hydrolyzed, and the KCNQ2/3 tail current was further inhibited (Fig. 3D). Together, the results suggest that roughly 30% (summary histogram, Fig. 3C) of the PM PI(4,5)P$_2$ pool is derived from a Golgi PI(4)P pool.

We tested whether depleting PI(4)P simultaneously at the PM and the Golgi would have a more powerful effect, giving more full inhibition of KCNQ2/3 tail currents. For these experiments we transiently cotransfected two anchors, PM LDR-CFP and Tgn38-FRB-CFP, along with PJ-4P and KCNQ2/3 (Table 1 and Fig. 4A). Separate confocal experiments confirmed that PJ-4P was initially cytosolic and that it was recruited to both anchors following rapamycin application (Fig. S3). In the electrophysiology experiments, we found that rapamycin recruited cytosolic PJ-4P to both anchors, increasing the FRET$_r$, and that KCNQ2/3 tail currents were strongly reduced (Fig. 4B, black line; ~75% reduction; $\tau = $ ~100 s). Evidently PI(4)P pools of the PM and of the Golgi together contribute the majority of PI(4)P needed for maintenance of PM PI(4,5)P$_2$.

Inhibiting PI 4-Kinases Reduces KCNQ2/3 Current. PI(4)P is synthesized from PI by type II and type III PI 4-kinases (1). We asked whether both classes of PI 4-kinase contribute precursor PI(4)P that ultimately enters the PM PI(4,5)P$_2$ pool. As general blockers of each class of PI 4-kinase, we used the type IIα and type IIβ inhibitor cytosolic adenosine (25, 44) and the type IIIα and type
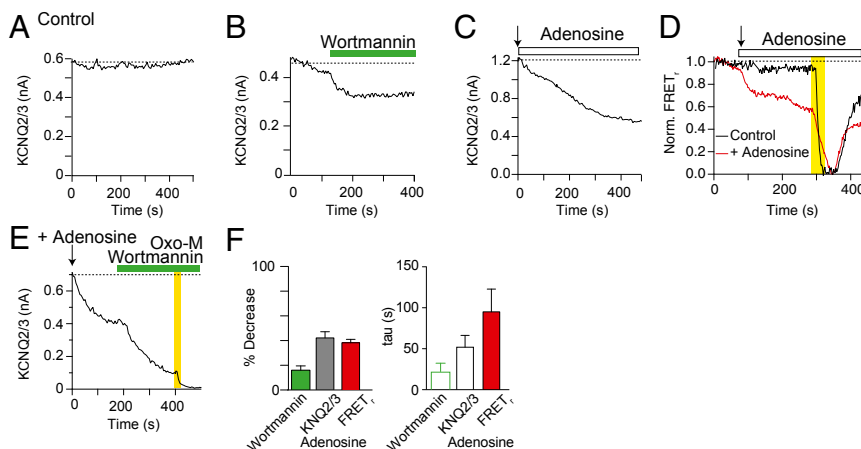
IIIβ inhibitor wortmannin. PI 4-kinase type IIIα localizes to the PM and makes significant contributions toward cellular PI(4,5)P$_2$ (13, 14, 16, 23, 30, 45). In control experiments, the KCNQ2/3 current is quite stable during 500 s of whole-cell recording (Fig. 5A). Application of wortmannin (30 μM) to block the type III kinases reduced the current by ~15% within a minute (Fig. 5B, summarized in F). Dialysis of adenosine (500 μM) through the patch pipette to block type II kinases was more effective, immediately initiating a slow ($\tau = $ ~50 s), ~40% reduction of KCNQ2/3 currents (Fig. 5 C and E, summarized in F). To verify that adenosine actually was acting on phosphoinositide metabolism, we asked whether it also reduces FRET$_r$ between CFP-PH$_{PLC\delta1}$ and YFP-PH$_{PLC\delta1}$, a photometric measure of PI(4,5)P$_2$. Similar to the results with KCNQ2/3 channels, application of adenosine through the patch pipette reduced FRET$_r$ between CFP-PH$_{PLC\delta1}$ and YFP-PH$_{PLC\delta1}$ (red line in Fig. 5D, summarized in F). We suggest that the adenosine-mediated reduction of KCNQ2/3 current and FRET$_r$ is through inhibition of PI 4-kinase activity and subsequent reduction of PM PI(4,5)P$_2$. When wortmannin (30 μM) was applied following the application of adenosine, KCNQ2/3 currents declined further to 90% inhibition (Fig. 5E). Thus, in steady-state, quiescent cells, both 4-kinase activities make a contribution, but the type II enzyme activity seems to be more important than type III activity to maintain KCNQ2/3 currents and the PM PI(4,5)P$_2$ pool.

Disrupting the Golgi or Inhibiting Myosin II ATPase Activity Reduces KCNQ2/3 Currents. Continuing our analysis of the significance of the Golgi for maintaining PM PI(4,5)P$_2$, we tested the effect of brefeldin A (BFA) on KCNQ2/3 currents and on the localization of YFP-PH$_{PLC\delta1}$. BFA is an inhibitor of Arf1 that disrupts transport from the endoplasmic reticulum to the Golgi by (i) collapsing the Golgi back into the ER, where (ii) endogenous ER-resident Sac1 effectively depletes PI(4)P. As reported by others (14), we found that treatment with BFA leads to rapid release of PI(4)P PH domains from the Golgi complex and disruption of the Golgi (Fig. S4). Hence, we reasoned that treatment with BFA might have similar effects on KCNQ2/3 currents or PM YFP-PH$_{PLC\delta1}$ intensity as recruitment of PJ-Sac to the Golgi. Indeed, application of 5 μg/mL BFA decreased both KCNQ2/3 currents (Fig. 6A) and the intensity of YFP-PH$_{PLC\delta1}$ measured over an entire total internal reflection fluorescence (TIRF) footprint (Fig. 6C) by ~20% (quantified in Fig. 6F). The presence of BFA did not alter (i) the further inhibition of KCNQ2/3 current or decrease in YFP-PH$_{PLC\delta1}$ intensity by M$_1$R activation or (ii) their rates of recovery following M$_1$R activation. Applying wortmannin together with BFA led to a larger decrease in KCNQ2/3 currents than with BFA alone (Fig. 6E versus Fig. 6A).

Along similar lines, we tested the hypothesis that cytoskeletal-assisted vesicle transport helps to replenish or maintain the PM pool of PI(4,5)P$_2$. We first disrupted myosin II motors with the general myosin II ATPase antagonist 2,3-butanedione monoxime (BDM; 20 mM). BDM slowly ($\tau = $ ~175 s; $n = 7$) decreased KCNQ2/3 currents by ~30% (Fig. 6 G and H). We next tested if the more specific myosin II ATPase inhibitor, blebbistatin (20 μM), had an effect on PM PI(4,5)P$_2$. Application of blebbistatin quickly decreased PM KCNQ2/3 currents by ~15% (Fig. 6 I and L). The blebbistatin-mediated fall in KCNQ2/3 currents was not accompanied by any statistically significant change of whole-cell membrane electrical capacitance, a measure of PM surface area. The experimental change was $-3 \pm 2\%$ from a control capacitance of $C_m = 26 \pm 8$ pF. A decrease in cell capacitance would be predicted if one assumes that blebbistatin slows vesicular transport to the PM more than endocytosis. To ensure that the decrease in KCNQ2/3 currents with blebbistatin was due to a loss of PI(4,5)P$_2$, we also monitored YFP-PH$_{PLC\delta1}$ intensity at the PM. As for KCNQ2/3 currents, blebbistatin decreased the intensity of PH$_{PLC\delta1}$ at the PM (Fig. 6 J–L). The rate of fall of KCNQ2/3
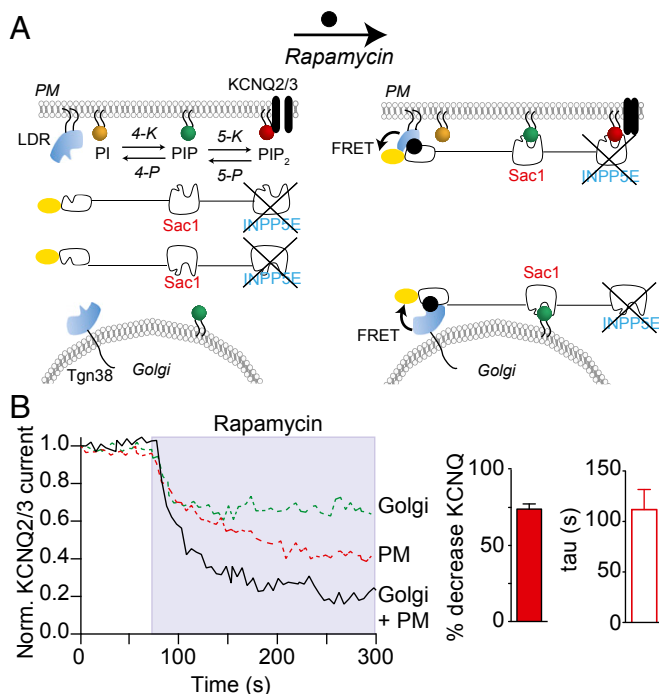
Fig. 4. Recruiting PJ-4P to the plasma membrane and simultaneously to the Golgi reduces KCNQ2/3 current in an additive manner. (A) Schematic of PJ-4P recruitment to both the plasma membrane and the trans-Golgi network. The INPP5E 5-phosphatase is inactivated, leaving only Sac1 4-phosphatase activity. (B) Averaged normalized time courses ($n = 5$) of KCNQ2/3 current with addition of 5 μM rapamycin. For comparison, data are plotted for recruitment to the Golgi (green line) or the plasma membrane (red line) alone. (Right) Summary of percentage decrease of KCNQ2/3 current and time constant (tau) of single-exponential fits.

Fig. 5. Inhibitors of type II and type III PI 4-kinases reduce plasma membrane PI(4,5)P$_2$. (*A*) Representative time course of KCNQ2/3 current in a control cell. (*B*) Time course of KCNQ2/3 current with addition of 30 μM wortmannin. (*C*) Time course of KCNQ2/3 current in a cell with 500 μM adenosine in the patch pipette solution. (*D*) Time course of FRET$_r$ between YFP-PH$_{PLC\delta1}$ and CFP- PH$_{PLC\delta1}$ in cells with (red line) or without (black line: control) 500 μM adenosine in the patch pipette solution. Arrow indicates transition from on-cell to whole-cell patch clamp configuration, beginning the dialysis of adenosine into the cell. Note that there is only a small change in FRET$_r$ after achieving "whole-cell" in control conditions, indicating that only a small amount of PH$_{PLC\delta1}$ has dialyzed out of the cell. Yellow bar marks the addition of 10 μM oxotremorine-M. M$_1$ muscarinic receptor is coexpressed. (*E*) Time course of KCNQ2/3 current in a cell with 1 mM adenosine in the pipette solution and bath exposure to 50 μM wortmannin and 10 μM oxotremorine-M. M$_1$ muscarinic receptor is coexpressed. (*F*) Summary of percentage decrease (*Left*) of KCNQ2/3 current and PH$_{PLC\delta1}$ intensity and time constant of single-exponential fit (*Right*) after addition of 30 μM wortmannin ($n = 8$) or 1 mM adenosine ($n = 10$).

currents following application of blebbistatin (Fig. 6*L*) was similar to that observed following PJ-4P recruitment to Tgn38 (Fig. 3*C*). Thus, the effects of BFA, BDM, and blebbistatin on KCNQ2/3 currents and PM YFP-PH$_{PLC\delta1}$ intensity are similar to those following recruitment of PJ-4P to the Golgi (Fig. 3 *C* and *D* versus Fig. 6 *A*, *G*, and *I*) and support the concept that some PI(4)P is continually being delivered to the PM, potentially through vesicular transport, to aid in the maintenance of PM PI(4,5)P$_2$.

Endogenous Sac1 Can Dephosphorylate Golgi PI(4)P. The PJ constructs contain truncated and engineered versions of the Sac-1 and INPP5E phosphatases that allow PJs to exist as soluble cytoplasmic proteins. On the other hand, full-length wild-type Sac1 is an integral membrane protein that localizes to nuclear and peripheral ER compartments in both yeast and mammals. During serum deprivation, Sac1 has been reported to traffic from the ER to the Golgi (6) and to down-regulate PI(4)P levels there. Recent studies have proposed that ER Sac1 also regulates PI(4)P at the PM (6, 36). To test whether endogenous mammalian ER Sac1 is capable of regulating PI(4)P in our system, we recruited ER membranes tagged with CFP-CB5-FKBP into apposition with the Golgi using the Golgi anchor Tgn38-FRB and rapamycin-induced dimerization (Table 1). At the same time, we monitored PI(4)P levels in the Golgi with PH$_{OSH1}$. Upon the addition of rapamycin, the PH$_{OSH1}$ intensity at the Golgi falls steadily (Fig. 7*A*, green line), whereas the mean intensity of the Golgi anchor (blue line) remains constant over the same area of interest. The decline of PH$_{OSH1}$ suggests that bringing the ER into apposition with the Golgi initiates dephosphorylation of PI(4)P to PI at the Golgi. The constancy of the Golgi anchor intensity shows that the measured decrease in Golgi PI(4)P reporter is not due to movement of the Golgi out of the region or focal plane of interest. We next tested the hypothesis that recruiting the ER to the Golgi would recapitulate the response of KCNQ2/3 currents to PJ-Sac recruitment to the Golgi. Indeed, recruiting the ER in apposition to the Golgi consistently resulted in a decrease in KCNQ2/3 currents at the PM (Fig. 7*B*). On average, KCNQ2/3 tail currents fell by ∼30%. The rate and total amount of reduction in KCNQ2/3 tail current was similar to that observed following recruitment of PJ-4P to the Golgi (compare Fig. 3*C* with Fig. 7*B*).

Discussion

We organize our discussion around the model of phosphoinositide pools shown in Fig. 7*C*. It represents a summary and working hypothesis about the relations of pools of PI, PI(4)P, and PI(4,5)P$_2$ in three organelles: PM, Golgi, and ER. In addition, it shows phosphoinositide transfer proteins (PITPs) that deliver PI to the PM (46) and a small, mobile organelle dubbed PIPerosome that has been postulated to synthesize and deliver PI to several cellular compartments (47). Our experiments in tsA-201 cells show that (*i*) plasma membrane PI(4,5)P$_2$ levels are supported by at least two precursor pools of PI(4)P, one in the PM and the other in the Golgi; (*ii*) selectively depleting PI(4)P at either location immediately initiates a slow reduction of KCNQ2/3 current or PH probe intensity, suggesting that the PI(4)P contributions from both pools are dynamic and ongoing; (*iii*) the contribution of the PM PI(4)P pool seems greater than that of the Golgi; (*iv*) translocating a 5-phosphatase to the Golgi has no effect on KCNQ2/3 currents, suggesting that the Golgi has no significant PI(4,5)P$_2$ pool; (*v*) inhibiting myosin II-mediated transport produces declines in PM PI(4,5)P$_2$ similar to those with depletion of Golgi PI(4)P, indicating continuous PI(4)P vesicular traffic from the Golgi to the PM; and (*vi*) endogenous Sac1 is capable of dephosphorylating Golgi PI(4)P and thus potentially acts as a regulator of PM PI(4,5)P$_2$.

Plasma Membrane and Golgi PI(4)P Maintain KCNQ2/3 Currents. We find that reducing PM PI(4)P, Golgi PI(4)P, or both simultaneously by PJ-4P results in a net reduction in KCNQ2/3 currents by ∼60, 30, and 75%, respectively. These decreases in KCNQ2/3 currents begin almost immediately in each case, suggesting that both pools are delivering lipid continuously, possibly in a cycle as a dynamic steady state. The concept that a Golgi pool of PI(4)P acts as a precursor for PM PI(4,5)P$_2$ is further bolstered by pharmacological experiments where disruption of the Golgi organelle, blockage of myosin motors, and inhibition of Golgi PI 4-kinase enzymatic activity reduce KCNQ2/3 current by ∼30%. The weight of evidence seems strong. In the simplest interpretation, ∼30% of PI(4)P responsible for generating PM PI(4,5)P$_2$ might traffic from the Golgi, whereas ∼60% might be generated de novo at the plasma membrane. However, this quantitative
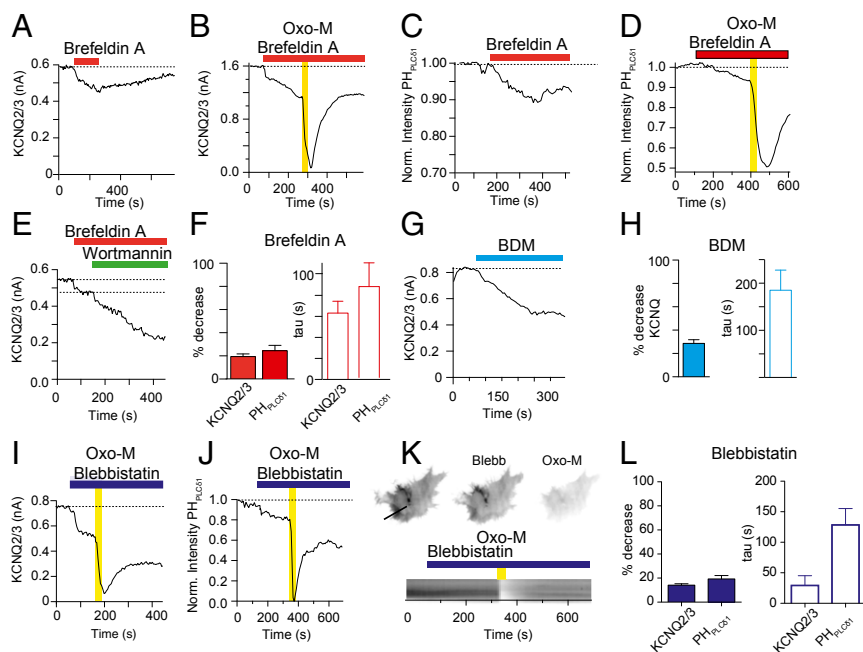
Fig. 6. Inhibitors of Golgi trafficking or myosin II ATPase activity reduce PM PI(4,5)P₂. (*A*) Time course of KCNQ2/3 current with addition of 5 μg/mL BFA. (*B*) As in *A*, with addition of 10 μM oxotremorine-M, M₁R is overexpressed. (*C*) Time course of normalized YFP-PH_PLCδ1 intensity within a TIRF footprint following the addition of BFA. (*D*) As in *C*, with the addition of the muscarinic agonist, Oxo-M (10 μM), M₁R is overexpressed. (*E*) As in *A* and *B*, with the addition of 30 μM wortmannin. (*F*) Summary of percentage decrease (*Left*) and time constant of single-exponential fit (*Right*) of KCNQ2/3 current and YFP-PH_PLCδ1 intensity after BFA alone (KCNQ2/3: *n* = 10; YFP-PH_PLCδ1: *n* = 6). Note that the percentage change in YFP-PH_PLCδ1 intensity is normalized to Oxo-M response. (*G*) Time course of KCNQ2/3 current with addition of 20 mM BDM. (*H*) Summary of percentage decrease of KCNQ2/3 current (*Left*) and time constant of single-exponential fit (*Right*) after addition of 20 mM BDM (*n* = 7). (*I*) Time course of KCNQ2/3 current following the addition of blebbistatin (30 μM) and Oxo-M (10 μM). (*J*) Time course of normalized YFP-PH_PLCδ1 intensity within a TIRF footprint following the addition of blebbistatin and Oxo-M. (*K*) Same cell as in *J*. (*Upper*) Inverted TIRF footprints from a cell expressing YFP-PH_PLCδ1 before, during, and after blebbistatin and Oxo-M. (*Lower*) Kymograph of YFP-PH_PLCδ1 intensity taken from black line. (*L*) Summary of percentage decrease (*Left*) and time constant of single-exponential fit (*Right*) of KCNQ2/3 current and YFP-PH_PLCδ1 intensity after blebbistatin alone (KCNQ2/3: *n* = 5; YFP-PH_PLCδ1: *n* = 10). Note that the percentage change in YFP-PH_PLCδ1 intensity is normalized to the Oxo-M response.

interpretation must be tempered by several possibilities. First, depletion in one of these compartments might accelerate synthesis or delivery from the other, partially masking the full effect (48–51). Second, PM-targeted PJ-4P likely can act on PI(4)P in the PM regardless of its source (i.e., synthesized at the PM or coming from the Golgi pool), thereby reporting the combined effect of both PI(4)P sources. Third, it is possible that Golgi-targeted PJ-4P also acts at points distal from the Golgi, thereby over-estimating the pool of PI(4)P present in this organelle. Such a compartment would be expected to contain PI(4)P and ultimately traffic to the PM.

Our results are consistent with previous evidence for precursor sources for PM PI(4,5)P₂ synthesis localized to the PM and the Golgi (28, 49, 52–54). For example, following transient activation of voltage-sensitive 5-phosphatase (49, 54), the recovery of PM PI(4,5)P₂ from its PM PI(4)P precursor is extremely fast (τ = ~10 s), suggesting that these pools normally may be in a rapid, dynamic equilibrium. Nevertheless, recent studies monitoring phosphoinositide levels by isotope labeling, mass spectrometry, and antibody staining in fixed cells have advanced the idea that the participation of PM PI(4)P pools in maintaining resting PM PI(4,5)P₂ is truly minor (29–31). Our experimental methods differ from theirs in that we record from single, living cells, monitor enzyme recruitment by FRET, and use KCNQ2/3 currents as a real-time readout of PM PI(4,5)P₂ levels. A likely explanation for these differences is that the various PI(4,5)P₂ sensors (PH domains, antibodies, KCNQ2/3 channels, and isotope labeling) have different sensitivities and different non-linearities and may not monitor identical pools of PM PI(4,5)P₂. There is also some evidence for signaling microdomains (55–57)

and independent pools of PI(4,5)P₂ (58, 59) in nanodomains (60, 61), possibilities that remain controversial (62).

Our experiments provide some temporal information. As measured by FRET, rapamycin-induced recruitment of enzymes to target anchors occurs in ~10 s. In about the same short time, recruiting PJ or PJ-5P to the PM can deplete nearly all of the PM PI(4,5)P₂, as reported by KCNQ2/3 channels and by PH_PLCδ1. This is a fast direct action of the enzymes. The 5-phosphatase can deplete the PI(4,5)P₂ pool in <10 s. By contrast, all of the actions of PJ-4P appear slow. They have 60- to 150-s time constants. This is true of the direct actions of PJ-4P, such as depletion of PI(4)P as measured by OSH1 and OSH2×2, as well as of the indirect ones, such as downstream changes of PI(4,5)P₂. Why are the direct actions so slow? We offer two reasons. The hypothesis we think most important is that the Sac1 4-phosphatase may be intrinsically much slower (lower catalytic rate constant) than the INPP5E 5-phosphatase so it takes much longer to deplete PI(4)P. This would apply to both the recruitable PJ-4P construct and the recruitable human Sac1 construct and may explain the slower rate of depletion at the PM versus the Golgi considering that the PM PI(4)P pool appears to be larger. The second concept would be that the OSH1 and OSH2×2 probes buffer PI(4)P and have long dwell times on PI(4)P. That would slow down the depletion of PI(4)P pools even by a fast enzyme. In this second scenario, the indirect downstream fall of PI(4,5)P₂ might also be slow in the absence of OSH probes because it requires that much time for PI(4)P pools to equilibrate with the PM PI(4,5)P₂ pool. However, it is useful to remember that the fast direct effects of PJ on PI(4,5)P₂ are seen here even in the presence of the buffering PH_PLCδ1 probe and that this probe has a dwell time on PI(4,5)P₂ that is as short as milliseconds (49). Furthermore, we
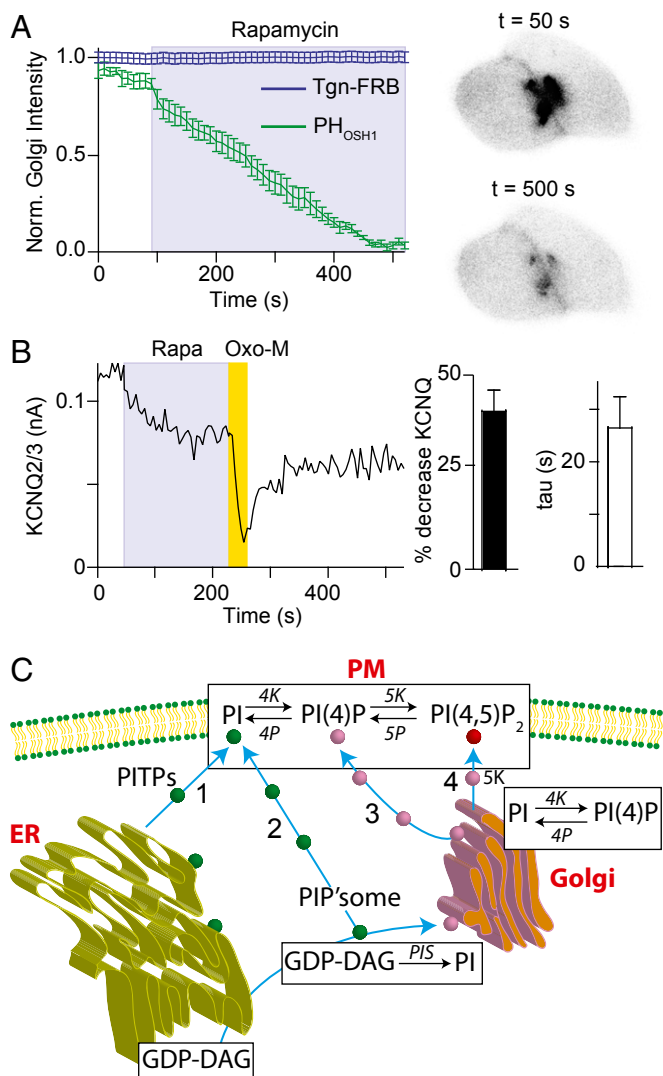
Fig. 7. Recruiting the endoplasmic reticulum to the Golgi depletes Golgi PI(4)P. (A) Averaged ($n = 7 \pm$ SEM) normalized time course of Golgi intensity of Tgn-FRB (blue line) and PH_{OSH1} (green line) with the addition of 5 μM rapamycin to recruit ER-localized CB5-FKBP in apposition to the Golgi. (*Right*) Confocal images of two cells with PH_{OSH1} before (*Upper*) and during (*Lower*) rapamycin. Tgn-FRB, *trans*-Golgi network-localized anchor; CB5-FKBP, chromogranin B5 bait localized to the endoplasmic reticulum. (*B*) Time course of KCNQ2/3 current with application of 5 μM rapamycin and 10 μM oxotremorine-M. M_1 muscarinic receptor is coexpressed. (*Right*) Summary of percentage decrease of KCNQ2/3 current and single-exponential time constant ($n = 8$). (*C*) Schematic of phosphoinositide synthesis via the plasma membrane, the endoplasmic reticulum, and the Golgi. GDP-DAG, GDP-diacylglycerol; PIS, phosphatidylinositol synthase; PIP'some, PIPerosome; PITPs, phosphatidylinositol transfer proteins. Blue arrows indicate transfer pathways of phosphatidylinositols between compartments; black arrows indicate phosphoinositide synthesis.

have previously shown that the PM PI(4)P pool can be phosphorylated by PI(4)P 5-kinase and transferred to the PM $PI(4,5)P_2$ pool in ~10 s (49, 63). Such observations favor the first hypothesis that the Sac1-containing constructs have a low enzyme velocity, although OSH probes must also be buffering $PI(4,5)P_2$. Thus, we suggest that the PM pool of $PI(4,5)P_2$ equilibrates more rapidly with the Golgi and PM PI(4)P than our 60- to 150-s time constants would suggest. Furthermore, if the PJ-4P enzyme is actually slow, then recruiting it may not deplete PI(4)P pools fully. Ongoing synthesis of PI(4)P may allow a modest amount of PI(4)P to remain in a dynamic steady state. For the same reason,

the fractional contribution of the Golgi and PM PI(4)P pools to the PM $PI(4,5)P_2$ pool may be underestimates.

Direct Delivery of $PI(4,5)P_2$ to the Plasma Membrane? How should we envision delivery from the Golgi PI(4)P pool to the PM? Perhaps it occurs mostly by fusion of standard transport vesicles that traffic continuously from the Golgi to the PM. A simple assumption would be that much of this traffic proceeds by the pathway labeled 3 in Fig. 7C, where PI(4)P is delivered directly into the PM PI(4)P pool. However, our results seem to require at least one other route. If we accept that the PJ-4P recruited to the PM depletes the PM pool of PI(4)P, then the enzyme should deplete PI(4)P that has come from the Golgi (pathway 3) as well as that which is synthesized de novo from PI at the PM. However, we find that recruiting PJ-4P to the PM and the Golgi simultaneously yields a greater reduction in KCNQ2/3 current than with recruitment to the PM alone. Our experiments suggest a significant contribution of PI(4)P from the Golgi to the PM occurring in a manner that is not sensitive to the PJ-4P recruited to the PM. This forces us to postulate another route, pathway 4, in which some vesicles initially containing PI(4)P transferring from the Golgi become associated with a 5-kinase so that their PI(4)P is converted to $PI(4,5)P_2$ before the vesicles arrive and fuse with the PM. Thus, by conversion en route, their cargo becomes immune to subsequent dephosphorylation by PJ-4P at the PM. Pathways 3 and 4 possibly represent the same physical vesicles—all of which, by encountering at least weak 5-kinase activity before fusing at the PM, deliver both PI(4)P and newly produced $PI(4,5)P_2$. In any case, we find remarkable that a transport mechanism that may involve vesicle trafficking can equilibrate lipid in a time as short as 1 min.

If the hypothesis of pathway 4 is correct, we expect the Golgi-derived transport vesicles to associate with a PI(4)P 5-kinase, possibly similar to the one recently identified in endosomes (64). We consider it unlikely that $PI(4,5)P_2$ is generated at the *trans*-Golgi network before trafficking as recruitment of the 5-phosphatase PJ-5P to the *trans*-Golgi resulted in little change in KCNQ2/3 currents. It is noteworthy that ~25% of KCNQ2/3 current remains when PJ-4P is recruited to both the PM and the Golgi. Is it possible that some PI(4)P in one of these compartments is inaccessible to PJ-4P, or that the slow Sac1 enzyme is always balanced by significant PI(4)P synthesis, or that PI(4)P from yet another location contributes to PM $PI(4,5)P_2$ production?

PI 4-Kinases and Myosin II-Mediated Transport Participate in the Maintenance of KCNQ2/3 Currents. Using PI 4-kinase inhibitors allowed us to probe the identity of PI 4-kinases involved in maintaining PM $PI(4,5)P_2$. Adenosine targets both PI4KII types α and β isoforms, whereas wortmannin inhibits PI4KIII types α and β. Inhibition of either PI4KII or PI4KIII enzymes reduces KCNQ2/3 currents (40% with adenosine, 15% with wortmannin). PI4KIIα, originally cloned from chromaffin granules (24), traffics throughout secretory pathways and has been suggested to be present in the *trans*-Golgi network, endosomes, and transport vesicles (26, 65–67); PI4KIIβ is found in the cytosol, trafficking vesicles, and clathrin-coated vesicles (68–70). Taking into account the apparent localization of PI4KII isoforms along different stages of the secretory pathway, it is logical that addition of adenosine has similar effects on PM $PI(4,5)P_2$ as depletion of the *trans*-Golgi PI(4)P pool (compare Fig. 3C versus Fig. 5 C and F). PI4KIII types α and β are present in the cytoplasm, plasma membrane, the Golgi, and the nucleolus. Considering the importance of PI4KIIIα in maintaining PM PI(4)P (16) and its potent inhibition by wortmannin (44, 45), the small size of the wortmannin effect on KCNQ2/3 currents (only a 15% decrease) is more puzzling. One possible explanation would be that following PI4KIII inhibition there is a compensatory slowing of lipid phosphatases. Two candidate enzymes are $PI(4,5)P_2$ 5-phosphatase

and PI(4)P 4-phosphatase. Reduction in the dephosphorylation rates might preserve PM PI(4,5)P_2 despite reduced precursor pools. When both sets of PI4K enzymes are inhibited, current is virtually eliminated. Unfortunately, these experiments still fall short of providing clear insight into the locations of the enzyme subtypes relative to the PI(4)P pools.

Further pharmacological analysis revealed that treatment with inhibitors of myosin II ATPase activity (BDM or blebbistatin) or disruption of the integrity of the Golgi (BFA) reduce PM PI(4,5)P_2 in a similar way as recruitment of PJ-4P to the Golgi. The near immediate, slow, ~20% reduction in KCNQ2/3 current or $PH_{PLC\delta1}$ intensity at the PM suggests that the contribution of Golgi PI(4)P is ongoing and that PI(4,5)P_2 production is coupled to membrane trafficking.

Endogenous ER Sac1 Can Dephosphorylate Golgi PI(4)P. Exposing the Golgi to endogenous Sac1 presented by the ER membrane inhibits PM KCNQ2/3 channels in a manner similar to recruiting cytosolic PJ-4P to the Golgi (compare Fig. 3C and Fig. 7B). Therefore, we believe that Sac1 resident on ER membranes is sufficient to reduce Golgi PI(4)P substantially. This accords with previous observations that Sac1 regulates PI(4)P levels at PM/ER contact sites (36) as well as possibly by trafficking to the Golgi (6, 7). PI(4)P has been shown to rise at the PM following inactivation of Sac1 (35) or following knockout of PM–ER contact sites (38). Such observations lead to the concept that Sac1 is a cellular "thermostat" controlling PM and Golgi PI(4)P levels.

Recapitulation. We return to the working hypothesis in Fig. 7C, a scheme strongly dependent on prior work extensively summarized by Balla (1). It shows three organelles: ER, Golgi, and PM, each with its own lipid pools, and enzyme activities that maintain the pool of PI(4,5)P_2 at the PM. We deduce that the PM pool of PI(4,5)P_2 needed to maintain KCNQ2/3 currents depends on at least two precursor pools of PI(4)P in the cell: one in the PM and the other in the Golgi. The PM pool seems to make the larger contribution. PI (dark green in Fig. 7C), produced in the ER and in PIPerosomes by PI synthase (47), is delivered by transfer proteins (pathway 1) and perhaps by highly mobile PIPerosomes to the PM (pathway 2) and to the Golgi. It should be noted that the putative PIPerosomes have not as yet been shown to make contact with the PM. PI 4-kinases in the Golgi and PM then produce pools of PI(4)P in both compartments. The Golgi pool of PI(4)P supplements the PM pool of PI(4)P directly but also may be phosphorylated by a 5-kinase during transit and delivered as PI(4,5)P_2 to the PM. The PM PI(4,5)P_2 pool takes about a minute to adjust to recruitment of PJ-4P to either Golgi or PM. Quite possibly, the equilibration of PM PI(4,5)P_2 with the PI(4)P pools is much faster, and the slow overall time course reflects slow action of the Sac1 phosphatase on each PI(4)P pool. Translocating the ER to the Golgi mimics the effects of translocating Sac1 to the Golgi. The decrease in PM PI(4,5)P_2 when either ER Sac1 or PJ-4P is active at the Golgi suggests that phosphoinositide traffic from the Golgi is ongoing and does not wait until the PM is depleted. We offer a dynamic and quantitative view of the last stages of PI(4,5)P_2 production and expect to extend these methods to other stages of phosphoinositide turnover.

Materials and Methods

Cell Culture and Transfection Conditions. All experiments were conducted on tsA-201 cells cultured in DMEM (Gibco 11995) with 10% serum and 0.2% penicillin/streptomycin. Cells were transfected at ~75% confluency with 0.2–1 μg of DNA using LipofectAmine 2000 (Invitrogen) and then either subcultured immediately (confocal experiments) or 24 h later (patch/photometry experiments) onto poly-ᴅ-lysine–coated cover-glass chips (#0; Thomas Scientific).

Confocal and TIRF Microscopy. One day posttransfection, cells were transferred from culture medium to a recording chamber containing modified Krebs–Ringer solution (see below for solution composition). Fluorophores were excited with an argon-ion (CFP, GFP, and YFP) and a helium-neon (RFP) laser and monitored using an inverted microscope under a 63× oil-immersion objective (confocal: LSM 710, Carl Zeiss MicroImaging; TIRF: Nikon TiE microscope equipped with a Photometrics QuantEM camera, Nikon instruments). Time series images were taken every 5–10 s at room temperature (23 °C). We and others (28) note that the expression of anchors, phosphatases, and PH probes should be carefully checked and, when possible, minimal amounts of DNA transfected. To qualify for study, each cell had to possess the optimum measure and distribution of anchor (Tgn38-FRB-CFP for Golgi; LDR-CFP for plasma membrane), phosphatase (PJ constructs), and phosphoinositide indicator [PM PI(4,5)P_2: $PH_{PLC\delta1}$; PM PI(4)P: $PH_{OSH2\times2}$; Golgi PI(4)P: PH_{OSH1}]. Cells that showed perturbed morphology, no sign of positive translocation of lipid phosphatase to the designated membrane anchor, or no increase in FER_r between membrane anchor (donor) and lipid phosphatase (acceptor) were excluded from further analysis. All confocal images or time-series experiments were analyzed using ImageJ/Fiji (National Institutes of Health).

Simultaneous Electrophysiology and Photometric FRET Measurements. KCNQ2/3 currents were recorded in whole-cell, gigaseal voltage clamp configuration at room temperature (71). Recordings were made using an EPC9 amplifier with Patchmaster 2.35 software (HEKA). Cells were held at a holding potential of –60 mV, and 500-ms test pulses to –20 mV were given every 4 s. KCNQ2/3 tail currents were measured by comparing current at 50 and 400 ms after repolarization to –60 mV using a custom-written algorithm (IGOR PRO software 6.0, Wavemetrics). In many experiments where rapamycin should induce translocation to a membrane anchor, we monitored this translocation by photometry as an increase in FRET between the enzyme (acceptor) and the membrane anchor (donor) (49). Membrane electrical capacitance was measured using the lock-in extension of the Patchmaster online program.

Materials and Solutions. All experiments were recorded in a 100-μL chamber continuously superfused (1 mL/min) with Ringer's solution containing (in mM): 160 NaCl, 2.5 KCl, 2 $CaCl_2$, 1 $MgCl_2$, 10 Hepes, 8 glucose, pH 7.4 (NaOH). Rapamycin, wortmannin (both from LC laboratories), oxotremorine, BFA, and blebbistatin (Sigma) were applied in the superfusate. BSA (1 mg/mL) was added as a carrier to all BFA-containing solutions. ᴅ-Myo-phosphatidylinositol 5-phosphate (Echelon) and adenosine (Sigma) were applied to the cell via a patch pipette.

Analysis and Statistics. All data were analyzed using Igor Pro software or ImageJ. Means are shown ± SEM, and significance is assessed by Student t test using GraphPad Prism software. Differences were considered significant when $P < 0.05$. Summarized data include one data point per cell.

1. Balla T (2013) Phosphoinositides: Tiny lipids with giant impact on cell regulation. *Physiol Rev* 93(3):1019–1137.
2. Doughman RL, Firestone AJ, Anderson RA (2003) Phosphatidylinositol phosphate kinases put PI4,5P_2 in its place. *J Membr Biol* 194(2):77–89.
3. Majerus PW, York JD (2009) Phosphoinositide phosphatases and disease. *J Lipid Res* 50(Suppl):S249–S254.
4. Di Paolo G, De Camilli P (2006) Phosphoinositides in cell regulation and membrane dynamics. *Nature* 443(7112):651–657.
5. Zhao X, et al. (2001) Interaction of neuronal calcium sensor-1 (NCS-1) with phosphatidylinositol 4-kinase β stimulates lipid kinase activity and affects membrane trafficking in COS-7 cells. *J Biol Chem* 276(43):40183–40189.

6. Blagoveshchenskaya A, et al. (2008) Integration of Golgi trafficking and growth factor signaling by the lipid phosphatase SAC1. *J Cell Biol* 180(4):803–812.
7. Faulhammer F, et al. (2007) Growth control of Golgi phosphoinositides by reciprocal localization of sac1 lipid phosphatase and pik1 4-kinase. *Traffic* 8(11):1554–1567.
8. Mesmin B, et al. (2013) A four-step cycle driven by PI(4)P hydrolysis directs sterol/PI(4)P exchange by the ER-Golgi tether OSBP. *Cell* 155(4):830–843.
9. Suh BC, Hille B (2008) PIP$_2$ is a necessary cofactor for ion channel function: How and why? *Annu Rev Biophys* 37:175–195.
10. Suh BC, Hille B (2002) Recovery from muscarinic modulation of M current channels requires phosphatidylinositol 4,5-bisphosphate synthesis. *Neuron* 35(3):507–520.

11. Zhang H, et al. (2003) PIP$_2$ activates KCNQ channels, and its hydrolysis underlies receptor-mediated inhibition of M currents. *Neuron* 37(6):963–975.
12. Winks JS, et al. (2005) Relationship between membrane phosphatidylinositol-4,5-bisphosphate and receptor-mediated inhibition of native neuronal M channels. *J Neurosci* 25(13):3400–3413.
13. Balla A, Balla T (2006) Phosphatidylinositol 4-kinases: Old enzymes with emerging functions. *Trends Cell Biol* 16(7):351–361.
14. Balla A, Tuymetova G, Tsiomenko A, Várnai P, Balla T (2005) A plasma membrane pool of phosphatidylinositol 4-phosphate is generated by phosphatidylinositol 4-kinase type-III alpha: Studies with the PH domains of the oxysterol binding protein and FAPP1. *Mol Biol Cell* 16(3):1282–1295.
15. Balla A, et al. (2008) Maintenance of hormone-sensitive phosphoinositide pools in the plasma membrane requires phosphatidylinositol 4-kinase IIIα. *Mol Biol Cell* 19(2):711–721.
16. Nakatsu F, et al. (2012) PtdIns4P synthesis by PI4KIIIα at the plasma membrane and its impact on plasma membrane identity. *J Cell Biol* 199(6):1003–1016.
17. Wong K, Meyers R, Cantley LC (1997) Subcellular locations of phosphatidylinositol 4-kinase isoforms. *J Biol Chem* 272(20):13236–13241.
18. Nakagawa T, Goto K, Kondo H (1996) Cloning, expression, and localization of 230-kDa phosphatidylinositol 4-kinase. *J Biol Chem* 271(20):12088–12094.
19. de Graaf P, et al. (2002) Nuclear localization of phosphatidylinositol 4-kinase β. *J Cell Sci* 115(Pt 8):1769–1775.
20. Haynes LP, Thomas GM, Burgoyne RD (2005) Interaction of neuronal calcium sensor-1 and ADP-ribosylation factor 1 allows bidirectional control of phosphatidylinositol 4-kinase β and trans-Golgi network-plasma membrane traffic. *J Biol Chem* 280(7):6047–6054.
21. Godi A, et al. (1999) ARF mediates recruitment of PtdIns-4-OH kinase-β and stimulates synthesis of PtdIns(4,5)P$_2$ on the Golgi complex. *Nat Cell Biol* 1(5):280–287.
22. Willars GB, Nahorski SR, Challiss RA (1998) Differential regulation of muscarinic acetylcholine receptor-sensitive polyphosphoinositide pools and consequences for signaling in human neuroblastoma cells. *J Biol Chem* 273(9):5037–5046.
23. Nakanishi S, Catt KJ, Balla T (1995) A wortmannin-sensitive phosphatidylinositol 4-kinase that regulates hormone-sensitive pools of inositolphospholipids. *Proc Natl Acad Sci USA* 92(12):5317–5321.
24. Barylko B, et al. (2001) A novel family of phosphatidylinositol 4-kinases conserved from yeast to humans. *J Biol Chem* 276(11):7705–7708.
25. Balla A, Tuymetova G, Barshishat M, Geiszt M, Balla T (2002) Characterization of type II phosphatidylinositol 4-kinase isoforms reveals association of the enzymes with endosomal vesicular compartments. *J Biol Chem* 277(22):20041–20050.
26. Waugh MG, et al. (2003) Localization of a highly active pool of type II phosphatidylinositol 4-kinase in a p97/valosin-containing-protein-rich fraction of the endoplasmic reticulum. *Biochem J* 373(Pt 1):57–63.
27. Minogue S, et al. (2006) Phosphatidylinositol 4-kinase is required for endosomal trafficking and degradation of the EGF receptor. *J Cell Sci* 119(Pt 3):571–581.
28. Szentpetery Z, Várnai P, Balla T (2010) Acute manipulation of Golgi phosphoinositides to assess their importance in cellular trafficking and signaling. *Proc Natl Acad Sci USA* 107(18):8225–8230.
29. Hammond GR, et al. (2012) PI4P and PI(4,5)P$_2$ are essential but independent lipid determinants of membrane identity. *Science* 337(6095):727–730.
30. Hammond GR, Schiavo G, Irvine RF (2009) Immunocytochemical techniques reveal multiple, distinct cellular pools of PtdIns4P and PtdIns(4,5)P$_2$. *Biochem J* 422(1):23–35.
31. Bojjireddy N, et al. (2014) Pharmacological and genetic targeting of the PI4KA enzyme reveals its important role in maintaining plasma membrane phosphatidylinositol 4-phosphate and phosphatidylinositol 4,5-bisphosphate levels. *J Biol Chem* 289(9):6120–6132.
32. Guo S, Stolz LE, Lemrow SM, York JD (1999) SAC1-like domains of yeast SAC1, INP52, and INP53 and of human synaptojanin encode polyphosphoinositide phosphatases. *J Biol Chem* 274(19):12990–12995.
33. Zhong S, et al. (2012) Allosteric activation of the phosphoinositide phosphatase Sac1 by anionic phospholipids. *Biochemistry* 51(15):3170–3177.
34. Yu JW, et al. (2004) Genome-wide analysis of membrane targeting by *S. cerevisiae* pleckstrin homology domains. *Mol Cell* 13(5):677–688.
35. Roy A, Levine TP (2004) Multiple pools of phosphatidylinositol 4-phosphate detected using the pleckstrin homology domain of Osh2p. *J Biol Chem* 279(43):44683–44689.
36. Stefan CJ, et al. (2011) Osh proteins regulate phosphoinositide metabolism at ER-plasma membrane contact sites. *Cell* 144(3):389–401.
37. Lindner M, Leitner MG, Halaszovich CR, Hammond GR, Oliver D (2011) Probing the regulation of TASK potassium channels by PI(4,5)P$_2$ with switchable phosphoinositide phosphatases. *J Physiol* 589(Pt 13):3149–3162.
38. Manford AG, Stefan CJ, Yuan HL, Macgurn JA, Emr SD (2012) ER-to-plasma membrane tethering proteins regulate cell signaling and ER morphology. *Dev Cell* 23(6):1129–1140.
39. Gozani O, et al. (2003) The PHD finger of the chromatin-associated protein ING2 functions as a nuclear phosphoinositide receptor. *Cell* 114(1):99–111.
40. Wang YJ, et al. (2003) Phosphatidylinositol 4 phosphate regulates targeting of clathrin adaptor AP-1 complexes to the Golgi. *Cell* 114(3):299–310.
41. Godi A, et al. (2004) FAPPs control Golgi-to-cell-surface membrane traffic by binding to ARF and PtdIns(4)P. *Nat Cell Biol* 6(5):393–404.
42. Manford A, et al. (2010) Crystal structure of the yeast Sac1: Implications for its phosphoinositide phosphatase function. *EMBO J* 29(9):1489–1498.
43. Ghosh RN, Mallet WG, Soe TT, McGraw TE, Maxfield FR (1998) An endocytosed TGN38 chimeric protein is delivered to the TGN after trafficking through the endocytic recycling compartment in CHO cells. *J Cell Biol* 142(4):923–936.
44. Tai AW, Bojjireddy N, Balla T (2011) A homogeneous and nonisotopic assay for phosphatidylinositol 4-kinases. *Anal Biochem* 417(1):97–102.
45. Downing GJ, Kim S, Nakanishi S, Catt KJ, Balla T (1996) Characterization of a soluble adrenal phosphatidylinositol 4-kinase reveals wortmannin sensitivity of type III phosphatidylinositol kinases. *Biochemistry* 35(11):3587–3594.
46. Chang CL, et al. (2013) Feedback regulation of receptor-induced Ca signaling mediated by E-Syt1 and Nir2 at endoplasmic reticulum-plasma membrane junctions. *Cell Rep* 5:813–825.
47. Kim YJ, Guzman-Hernandez ML, Balla T (2011) A highly dynamic ER-derived phosphatidylinositol-synthesizing organelle supplies phosphoinositides to cellular membranes. *Dev Cell* 21(5):813–824.
48. Xu C, Watras J, Loew LM (2003) Kinetic analysis of receptor-activated phosphoinositide turnover. *J Cell Biol* 161(4):779–791.
49. Falkenburger BH, Jensen JB, Hille B (2010) Kinetics of PIP$_2$ metabolism and KCNQ2/3 channel regulation studied with a voltage-sensitive phosphatase in living cells. *J Gen Physiol* 135(2):99–114.
50. Falkenburger BH, Dickson EJ, Hille B (2013) Quantitative properties and receptor reserve of the DAG and PKC branch of G$_q$-coupled receptor signaling. *J Gen Physiol* 141(5):537–555.
51. Chahwala SB, Fleischman LF, Cantley L (1987) Kinetic analysis of guanosine 5′-O-(3-thiotriphosphate) effects on phosphatidylinositol turnover in NRK cell homogenates. *Biochemistry* 26(2):612–622.
52. Suh BC, Inoue T, Meyer T, Hille B (2006) Rapid chemically induced changes of PtdIns(4,5)P$_2$ gate KCNQ ion channels. *Science* 314(5804):1454–1457.
53. Ueno T, Falkenburger BH, Pohlmeyer C, Inoue T (2011) Triggering actin comets versus membrane ruffles: Distinctive effects of phosphoinositides on actin reorganization. *Sci Signal* 4(203):ra87.
54. Halaszovich CR, Schreiber DN, Oliver D (2009) Ci-VSP is a depolarization-activated phosphatidylinositol-4,5-bisphosphate and phosphatidylinositol-3,4,5-trisphosphate 5′-phosphatase. *J Biol Chem* 284(4):2106–2113.
55. Delmas P, Brown DA (2002) Junctional signaling microdomains: Bridging the gap between the neuronal cell surface and Ca^{2+} stores. *Neuron* 36(5):787–790.
56. Zhang J, Bal M, Bierbower S, Zaika O, Shapiro MS (2011) AKAP79/150 signal complexes in G-protein modulation of neuronal ion channels. *J Neurosci* 31(19):7199–7211.
57. Zaika O, Zhang J, Shapiro MS (2011) Combined phosphoinositide and Ca^{2+} signals mediating receptor specificity toward neuronal Ca^{2+} channels. *J Biol Chem* 286(1):830–841.
58. Simonsen A, Wurmser AE, Emr SD, Stenmark H (2001) The role of phosphoinositides in membrane transport. *Curr Opin Cell Biol* 13(4):485–492.
59. Golebiewska U, et al. (2011) Evidence for a fence that impedes the diffusion of phosphatidylinositol 4,5-bisphosphate out of the forming phagosomes of macrophages. *Mol Biol Cell* 22(18):3498–3507.
60. Wang J, Richards DA (2012) Segregation of PIP$_2$ and PIP$_3$ into distinct nanoscale regions within the plasma membrane. *Biol Open* 1(9):857–862.
61. Fujita A, Cheng J, Tauchi-Sato K, Takenawa T, Fujimoto T (2009) A distinct pool of phosphatidylinositol 4,5-bisphosphate in caveolae revealed by a nanoscale labeling technique. *Proc Natl Acad Sci USA* 106(23):9256–9261.
62. van Rheenen J, Achame EM, Janssen H, Calafat J, Jalink K (2005) PIP$_2$ signaling in lipid domains: A critical re-evaluation. *EMBO J* 24(9):1664–1673.
63. Suh BC, Leal K, Hille B (2010) Modulation of high-voltage activated Ca^{2+} channels by membrane phosphatidylinositol 4,5-bisphosphate. *Neuron* 67(2):224–238.
64. Sun Y, Hedman AC, Tan X, Schill NJ, Anderson RA (2013) Endosomal type Iγ PIP 5-kinase controls EGF receptor lysosomal sorting. *Dev Cell* 25(2):144–155.
65. Weixel KM, Blumental-Perry A, Watkins SC, Aridor M, Weisz OA (2005) Distinct Golgi populations of phosphatidylinositol 4-phosphate regulated by phosphatidylinositol 4-kinases. *J Biol Chem* 280(11):10501–10508.
66. Clayton EL, Minogue S, Waugh MG (2013) Mammalian phosphatidylinositol 4-kinases as modulators of membrane trafficking and lipid signaling networks. *Prog Lipid Res* 52(3):294–304.
67. Burgess J, et al. (2012) Type II phosphatidylinositol 4-kinase regulates trafficking of secretory granule proteins in Drosophila. *Development* 139(16):3040–3050.
68. Jung G, et al. (2008) Molecular determinants of activation and membrane targeting of phosphoinositol 4-kinase IIβ. *Biochem J* 409(2):501–509.
69. Jung G, et al. (2011) Stabilization of phosphatidylinositol 4-kinase type IIβ by interaction with Hsp90. *J Biol Chem* 286(14):12775–12784.
70. Li J, et al. (2012) Molecular brightness analysis reveals phosphatidylinositol 4-kinase IIβ association with clathrin-coated vesicles in living cells. *Biophys J* 103(8):1657–1665.
71. Dickson EJ, Falkenburger BH, Hille B (2013) Quantitative properties and receptor reserve of the IP$_3$ and calcium branch of G$_q$-coupled receptor signaling. *J Gen Physiol* 141(5):521–535.